Journal of Sciences, Islamic Republic of Iran 29(4): 311 – 319 (2018) http://jsciences.ut.ac.ir
University of Tehran, ISSN 1016-1104

Expedient Catalytic Access to Geraniol Epoxide Using a New Vanadium Schiff Base Complex on Modified Magnetic Nanoparticles

F. Farzaneh*, and E. Rashtizadeh

Department of Chemistry, Faculty of Physics and Chemistry, Alzahra University P.O.Box 1993891176, Vanak, Tehran, Islamic Republic of Iran

Received: 22 November 2017 / Revised: 6 March 2018 / Accepted: 8 April 2018

Abstract

The Fe_3O_4@SiO_2@APTMS@Glu-His@V complex was prepared with modification of iron oxide magnetic nanoparticles with (3-aminopropyl) trimethoxysilane (APTMS) and glutaraldehyde-L-histidine Schiff base followed by complexation with $VOSO_4$. Characterization of the Fe_3O_4@SiO_2@APTMS@Glu-His@V complex was carried out by means of FTIR, XRD, SEM, EDX, TEM, AAS and VSM techniques. It was found that Fe_3O_4@SiO_2@APTMS@Glu-His@V complex successfully catalyze the epoxidation of allyl alcohols with tert-butylhydroperoxide (TBHP) in moderate to high yields. The epoxidation of geraniol with 100 % conversion and 100% selectivity within 15 min is remarkable. Short reaction time, high activity, selectivity, stability, reusability and easily magnetic separation of the catalyst with no leaching during the course of reactions are some advantages of this research.

Keywords: Nanoparticles; Epoxidation; Vanadium complex; Allylic alcohols.

Introduction

Epoxides are excellent starting materials for synthesis of several commercial products such as epoxy resin adhesives, coating materials, perfumes, plasticizers and medicinal products [1]. To find efficient method for catalytic epoxidation is an important goal in synthetic chemistry.

Some transition metal compounds prepared with, Ti, Fe, Co, Mn, Mo, Zr, Cr and V are known for their redox properties and their capacity to catalyze the epoxidation reactions [1]. Among these metals, vanadium complexes have attracted increasing attention due to specific catalytic, biological and medicinal properties [2-10]. Especially, the use of vanadium complexes in selective epoxidation of unsaturated hydrocarbons and allyl alcohols is a topic of great interest [11]. Vanadium behaving with many different oxidation states in coordination complexes makes it to show unusual redox ability. For example, vanadium acts as a strong Lewis acid in oxovanadium (IV) complexes due to low radius to charge ratio, with a high affinity for oxygen which can motivate various organic transformation reactions [11]. Recently much research have been focused on the coordination of vanadium complexes because of its interesting features in biological roles in a variety of biochemical processes such as phosphorylation [12], nitrogen fixation [13],

* Corresponding author: Tel: +982188258977; Fax: +982188041344; Email: faezeh_farzaneh@yahoo.com; farzaneh@alzahra.ac.ir

glycogen metabolism [14], insulin mimicking [15,16] and haloperoxidation [17-18]. The haloperoxides catalyze a variety of oxidation reactions such as oxidation of bromide to hypobromite or the epoxidation of olefins.

In recent years, the heterogenization of transition metal complexes through immobilization onto solid supports has received great attention due to the inherent advantages of shape selectivity, easy separation and recycling of catalysts, product purification, no corrosion and better handling properties [19-21]. Many strategies have been adopted to heterogenize the homogeneous catalysts by using solid supports like microporous [22-24] and mesoporous materials [25-32]. The utilization of magnetic nanoparticles as solid supports is interesting subject for study due to easily separation of products from the reaction medium by using an external magnet. This method improves the catalyst recovery, avoids losing it and increases its reusability during separation process in comparison to that of filtration or centrifugation. Therefore, there is a considerable reduction in operational cost. Moreover, nanocatalyst with large specific surface area and high catalytic activity also increases the catalytic efficiency [33-40].

In this work, attempts have been made to design a new heterogeneous catalyst for epoxidation of allyl alcohols. For this, a new Schiff base ligand with *L*-histidine and glutaraldehyde was prepared and then immobilized on magnetic nanoparticles followed by complexation with vanadium oxide ions (VO^{2+}).

Materials and Methods

All materials were of commercial reagent grade and used without further purification. $FeCl_2.4H_2O$, $FeCl_3.6H_2O$, 3-aminopropyltrimethoxysilane (APTMS), ammonium hydroxide solution 25% (w/w), glycerol, sodium silicate, hydrochloric acid, sodium chloride, *L*-histidine, acetonitrile, methanol, ethanol, chloroform, dichloromethane, TBHP solution 70 % in water, hydrogen peroxide solution 30% (w/w), diphenylamine, *trans*-2-hexen-1-ol, cinnamyl alcohol and 1-octen-3-ol, were purchased from Merck Chemical Company. Vanadyl sulfate and geraniol were obtained from Aldrich. Glutaraldehyde (50% W/V in water) was purchased from Sigma Alderich Chemical Company.

Characterization

The X-ray diffractions (XRD) patterns of samples were recorded on a Philips PW1800 diffractometer using monochromatic nickel-filtered Cu K_α radiation (k = 0.15405 nm). The X-ray generator was run at 40 kV and 30 mA and the diffractograms were recorded in the 2h range of 4°–90°. The phases were identified using the powder diffraction file (PDF) database (JCPDS, International Centre for Diffraction Data). Magnetic measurements were carried out using a Quantum Design vibrating sample magnetometer (VSM) at room temperature in an applied magnetic field sweeping from -8000 to 8000 O_e (BHV-55, Riken, Japan). Scanning electron microscopy (SEM) images were obtained on a Philips XL-30ESEM equipped with an X-ray energy dispersive detector (EDX) and transmission electron microscopy (TEM) images were taken by Zeiss-EM10C-100 KV. FTIR spectra of the samples were collected on a Bruker (Tensor 27) instrument in the range of 4000–400cm^{-1} (5 mg sample with 100 mg KBr) under the atmospheric condition. The chemical analysis was carried out with an atomic absorption Chermo double beam instrument. Epoxidation products were analyzed by GC and GC-Mass using Agilent 6890 series with a FID detector, HP-5, 5% phenylmethylsiloxane capillary and helium as carrier gas and Agilent 5973 network, mass selective detector, HP-5 MS 6989 network GC system.

Preparation of Fe_3O_4 magnetic nanoparticles (MNPs) and modified SCMNPs and (Fe_3O_4@SiO_2@APTMS)

These compounds were prepared according to the previously reported procedures [34].

Preparation of Schiff base (Glu-His)

The Schiff base was synthesized via modification of the previously reported procedure [35]. An aqueous solution of *L*-histidine (0.1 M, 0.155 g in 10 mL of deionized water) was added to glutaraldehyde (0.1 M, 0.094 mL in 10 mL of deionized water). The solution was then heated at 45°C for 2 h. The solution color changed from transparent to light yellow after 30 min and then to dingy which indicated the completion of the reaction and formation of the product (denoted as Glu-His).

Preparation of Fe_3O_4@SiO_2@APTMS@Glu-His

Immobilized Glu-His was prepared as reported [36] by adding the Fe_3O_4@SiO_2@APTMS (1.0 g) to Glu-His solution in H_2O (20 mL) and stirring at 80°C for 2 h for the formation of the Schiff base between Fe_3O_4@SiO_2@APTMS amino group and the free aldehyde of the Glu-His. The brown solid product was separated by means of an external magnet followed by washing with deionized water for several times.

Preparation of Fe_3O_4@SiO_2@APTMS@Glu-His@V complex

Fe_3O_4@SiO_2@APTMS@Glu-His (1.0 g) was added

to a solution of $VOSO_4$ (0.06 M in deionized water, 20 mL) and the resultant mixture stirred at 80°C for 8 h. The solid product was then separated, washed with water for several times and dried in air.

Catalytic epoxidation, general procedure

All epoxidation reactions of the allyl alcohols (geraniol, cinnamyl alcohol, *trans*-2-hexen-1-ol and 1-octene-3-ol) were carried out in a round bottom flask equipped with a magnetic stirrer and a water-cooled condenser. Typically, the desired amount of catalyst, substrate (10.0 mmol), solvent (5 mL) and TBHP (12 mmol) were added to the reaction flask and the mixture heated at reflux for an appropriate amount of time. Separation of the catalyst was carried out by means of an external magnet. The progress of reaction was monitored by GC and the products were characterized by GC-Mass.

Results and Discussion

Catalyst characterization

Fe_3O_4@SiO_2@APTMS@Glu-His@V complex was prepared according to the reaction sequences presented in Scheme 1. MNPs, SCMNP and AmpSCMNPs were prepared as reported [34]. Then, Schiff base ligand prepared from glutaraldehyde and histidine and designated as Glu-His was immobilized on the surface of AmpSCMNP through reaction of amine group of AmpSCMNPs with Glu-His [35, 36]. In the final step, complexation of Fe_3O_4@SiO_2@APTMS@Glu-His with $VOSO_4.3H_2O$ afforded the Fe_3O_4@SiO_2 @APTMS@Glu-His@V complex nanomaterials (Scheme 1).

Helpful information about the success of the immobilization process can be obtained from infrared spectroscopy. This objective can be achieved by comparison of the MNP spectrum with that of the modified surface. The FT-IR spectrum of Fe_3O_4 which is shown in Fig. 1a demonstrates bands appearing at 448 and 579 cm^{-1} due to the Fe-O vibrations. After coating of Fe_3O_4 with silica, appearance of a new peak at 1090 cm^{-1} indicates the formation of Si-O bond on the Fe_3O_4 surface. Observation of the C–H stretching vibrations at 2855 and 2925 cm^{-1} in the spectrum obtained after functionalizing with APTMS confirms the occurrence of condensation reaction (Fig. 1c) [33-35].

The spectrum of the Schiff base Glu-His (Fig. 1d) shows a band at 1360 cm^{-1} for the C-N vibration. Likewise, whereas the rather strong band displaying at 1635 cm^{-1} is assigned to the C=N stretching vibration, the similar absorption for free aldehyde C=O is observed in 1728 cm^{-1}. The spectrum of the immobilized Schiff base presented in Fig. 1e indicates several changes in comparison to that of Fe_3O_4@SiO_2@APTMS (Fig. 1c). For example, the increase in the intensity of C=N and C-H stretching vibrations observed respectively at 1637 and 2865 and 2940 cm^{-1} is assigned to the Glu-His group bonded to Fe_3O_4@SiO_2@APTMS [36].

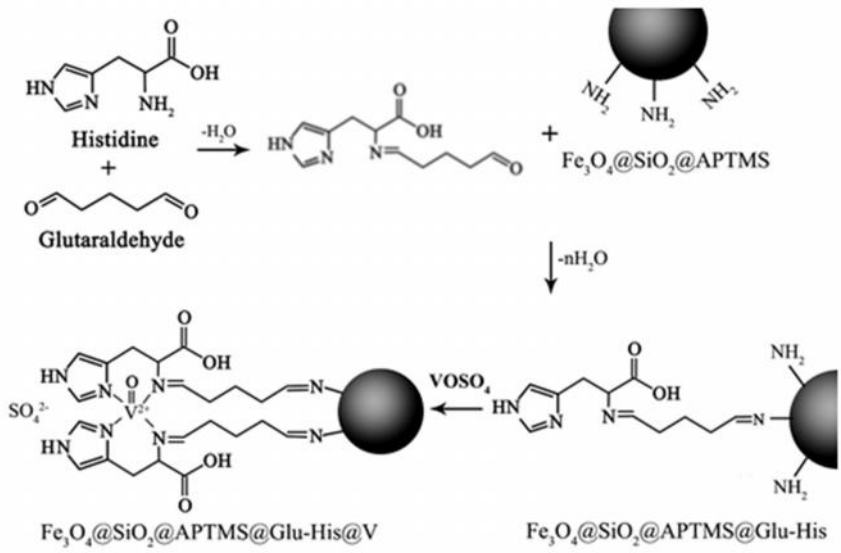

Scheme 1. Preparation of Fe_3O_4@SiO_2@APTMS@Glu-His@V complex.

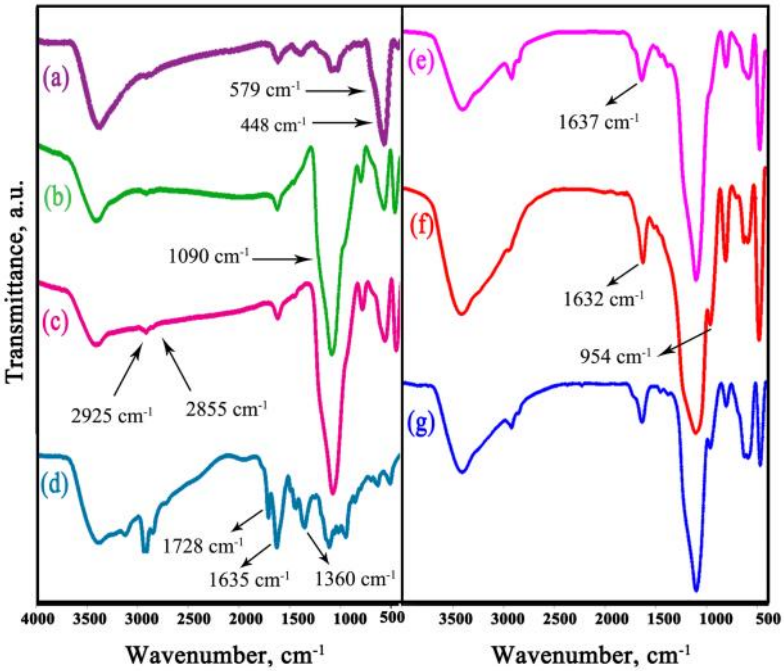

Figure 1. The FTIR spectra of (a) Fe_3O_4, (b) Fe_3O_4@SiO_2, (c) Fe_3O_4@SiO_2@APTMS, (d) Glu-His, (e) Fe_3O_4@SiO_2 @APTMS@Glu-His, (f) Fe_3O_4@SiO_2@APTMS@Glu-His@V complex before using and (g) after using as catalyst.

In addition, whereas the C=N stretching vibration of the Glu-His in the Fe_3O_4@SiO_2@APTMS@Glu-His spectrum appears at 1637 cm^{-1} (Fig. 1e), shifting to a lower wave number at 1632 cm^{-1} occurs when Fe_3O_4@SiO_2@APTMS@Glu-His@V complex is generated (Fig. 1f). A decrease of 5 cm^{-1} in C=N stretching which shows reduction of bond order confirms the coordination of the Schiff base nitrogen atom to the vanadium ion. In addition, the bands displaying at 954 cm^{-1} due to the V=O stretching vibrations within the range 960±50 cm^{-1} belong to the monomeric square pyramidal oxovanadium (IV) complexes [33-37].

The XRD patterns of the prepared Fe_3O_4@SiO_2@APTMS@Glu-His@V complex before and after using as catalyst are shown in Fig. 2a–b respectively. The diffraction peaks of Fe_3O_4@SiO_2@APTMS@Glu-His@V complex nanoparticles with d values appeared at 4.90, 2.95, 2.52, 2.08, 1.70, 1.60, 1.48, 1.27 and 1.11 are related to the (111), (220), (311), (400), (422), (511), (440), (533) and (444) planes (Fig. 2a). These results are consistent with JCPDS card No. 1-1111 and present the similarity of the iron oxide characteristic peaks with cubic structure. The similar set of characteristic peaks of Fe_3O_4@SiO_2@APTMS@Glu-His@V complex with iron oxide nanomagnet determine the stability of the Fe_3O_4 nanoparticle crystalline phase during silica coating and immobilization of Schiff base complex (Fig. 2a).

The SEM images of Fe_3O_4, Fe_3O_4@SiO_2@APTMS and Fe_3O_4@SiO_2@APTMS@Glu-His@V complex presented in Fig. 3A reveal that the particle sizes are 16, 20 and 25 nm respectively with spherical morphology. As such, an increase in the nanomagnet particle size after each immobilization is concluded.

Analysis of the EDX pattern of Fe_3O_4@SiO_2@APTMS@Glu-His@V complex presented in Fig. 3B confirms the presence of V, N, C, O, Si, and Fe. The average vanadium content was found

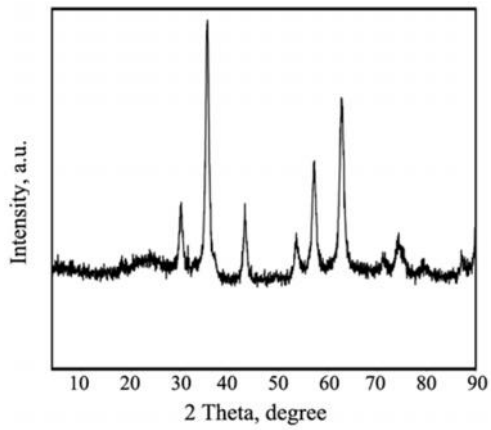

Figure 2. XRD pattern of Fe_3O_4@SiO_2@APTMS@Glu-His@V complex.

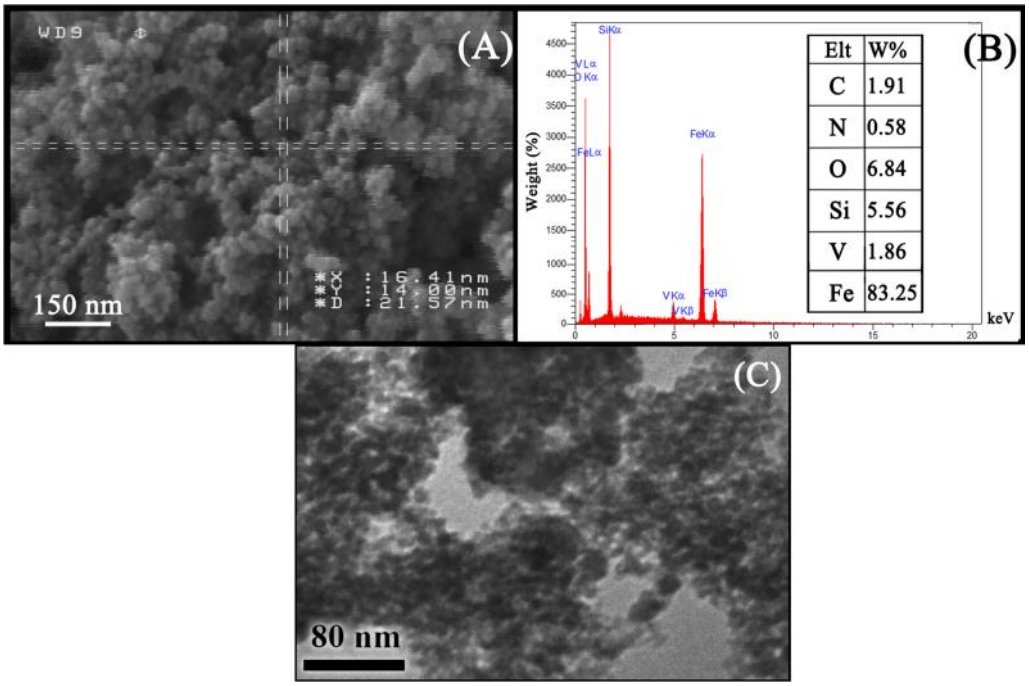

Figure 3. The SEM image of (a) Fe_3O_4@SiO_2@APTMS@Glu-His@V complex, (b) the EDX map of Fe_3O_4@SiO_2@APTMS@Glu-His@Vcomplex,and (c) The TEM image of Fe_3O_4@SiO_2@APTMS@Glu-His@Vcomplex.

to be 1.86%, consistent with the content obtained by atomic absorption determination (1.80%).

Based on the TEM results of Fe_3O_4@SiO_2@APTMS@Glu-His@V complex presented in Fig. 3C, observation of the core –shell nanomagnet is significant.

The VSM analysis of Fe_3O_4@SiO_2@APTMS@Glu-His@V complex before and after using as catalyst at 300K was carried out to demonstrate the magnetic properties. As indicated in Fig. 4, not only the VSM diagrams are seen for the prepared catalyst, but also both remanence and coerecivity are zero and no hysteresis is observed. Therefore, it can be concluded that catalyst is superparamagnetic [34]. The saturation magnetization value was determined to be 27 emu/g.

Catalyst activity

Geraniol was used as model substrate to study the catalytic performance of Fe_3O_4@SiO_2@APTMS@Glu-His@V complex in the epoxidation reaction using TBHP as oxidant (Scheme 2). In order to find the optimum reaction conditions, the effect of various reaction parameters such as the amount of catalyst, reaction time and solvent were evaluated.

As indicated in Fig. 5, determination of the geraniol conversion using 0.01 to 0.1 g of Fe_3O_4@SiO_2@APTMS@Glu-His@V complex as catalyst revealed that reaction proceeds to completion within 15 minutes if 0.1 g of catalyst is used. Therefore, other reactions were carried out using 0.1 g of the catalyst.

The influence of different solvents such as chloroform, acetonitrile, ethanol and dichloromethane at different times were investigated. As seen in this Fig. 6, a decrease in conversion is observed in the order of chloroform > dichloromethane > ethanol > acetonitrile. For example, whereas reaction proceeds to completion within 15 minutes in chloroform with dielectric constants of 4.8, only 60% of geraniol is converted within 60 minutes in acetonitrile with dielectric constants of 37 (Fig. 6). Since the solvent trend is in the opposite order of the increasing solvent dielectric constant, the higher catalyst reactivity in the less polar solvent is concluded.

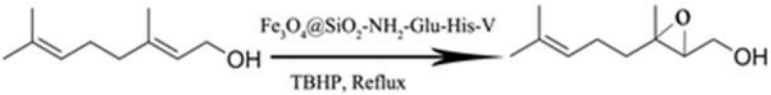

Scheme 2. Catalytic epoxidation of geraniol.

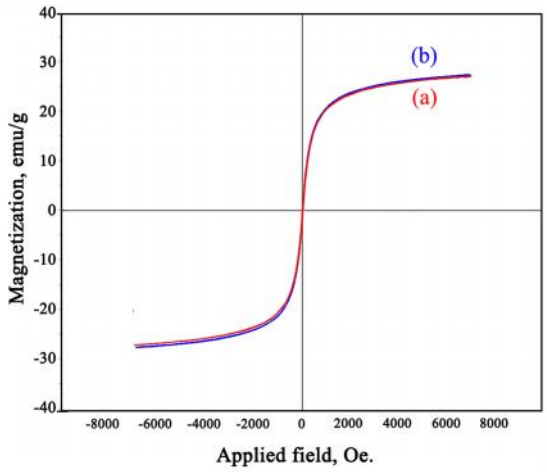

Figure 4. Magnetization curves of (a) Fe_3O_4@SiO_2@APTMS@Glu-His@V complex before and (b) after using as catalyst.

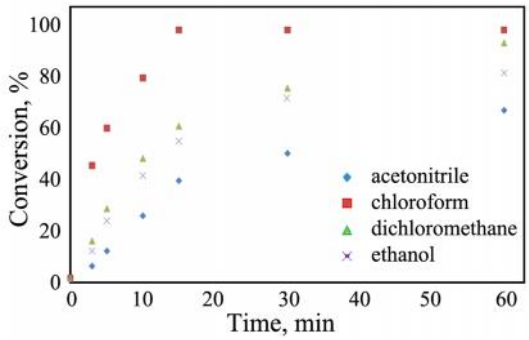

Figure 5. The effect of solvent at diffrenet time on the conversion of geraniol using Fe_3O_4@SiO_2@APTMS@Glu-His@V as catalyst. Reaction condition: 10 mmol geraniol, 12 mmol TBHP, 5 mL solvent, 0.1 g catalyst.

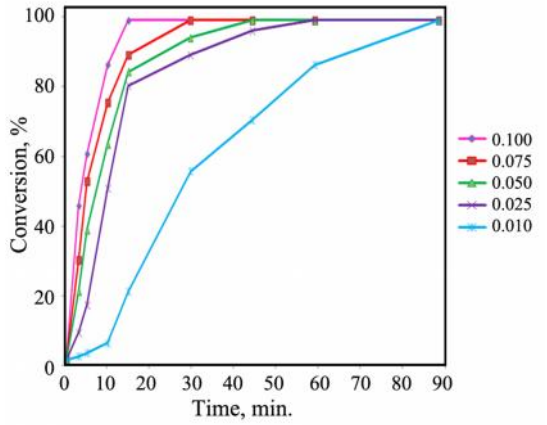

Figure 6. The effect of amount of Fe_3O_4@SiO_2@APTMS@Glu-His@V catalyst at diffrenet time on the conversion of geraniol. Reaction condition: 10 mmol geraniol, 12 mmol TBHP, 5 mL solvent, 0.1 g catalys and chloroform as solvent.

In order to determine the general applicability of the Fe_3O_4@SiO_2@APTMS@Glu-His@V catalyst, epoxidation reactions of other allyl alcohols including *trans*-2-hexen-1-ol, 1-octene-3-ol and cinnamyl alcohol were studied under optimized epoxidation conditions (Scheme 3 and Table 1). We have included the geraniol epoxidation in the presence of Fe_3O_4@SiO_2@APTMS in Scheme 3 and Table 1 in order to make the comparison with Fe_3O_4@SiO_2@APTMS@Glu-His@V more convenient. Whereas geraniol shows the highest activity when catalyzed with catalyst containing vanadium complex, only 3% of geraniol undergoes epoxidation using Fe_3O_4@SiO_2@APTMS which is void of complex. These results clearly indicate the key role of the vanadium Schiff base complex present on the modified iron nanoparticles as catalyst in the epoxidation reactions.

The catalyst reusability was examined by conducting catalytic tests on Fe_3O_4@SiO_2@APTMS@Glu-His@V complex under optimized epoxidation conditions. After completion of the reaction, the catalyst was filtered and washed with solvent and dried for using in another other reaction cycles. It was found that the recovered catalyst show good reactivity up to 4 cycles without significant loss in epoxidation yields (from 99 to 95%) (Fig. 7). The stability of the magnetically recovered Fe_3O_4@SiO_2@APTMS@Glu-His@V complex was also studied by recycling the recovered catalyst and determination of the vanadium content using atomic absorption spectroscopy. The vanadium contents of the fresh and used catalysts were determined to be 1.80 and 1.74%, respectively.

Finally, to investigate the heterogeneity character of the catalysis system, the catalyst was recovered by external magnet from reaction mixture after 4 min and reaction was then allowed to continue in the absence of catalyst. Observation of no change in the conversion before and after removing of the catalyst clearly indicated the heterogeneity character of the catalysis system. Moreover, the FTIR, XRD and VSM of Fe_3O_4@SiO_2@APTMS@Glu-His@V complex before and after using as catalyst shown respectively in Figures 1g, 2b, and 5b were found to be similar. Observation of the bands displaying at 995 cm^{-1} due to the V=O stretching vibrations in the FTIR spectrum of the used catalyst indicates the stability of vanadium present in the catalyst. The VSM diagrams showed that magnetic properties remained intact in both compounds. The XRD patterns also determined that Fe_3O_4 nanoparticle crystalline phase is stable during reaction.

Table 1. Results obtained for epoxidation of different allyl alcohols in the presence of Fe_3O_4@SiO_2@APTMS@Glu-His@V catalyst.

Entry	Substrate	Time (min)	Conversion (%)	Selectivity (%)	TOF
1	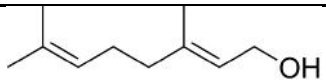 geraniol	3	45	100	1140
		5	60		
		10	86		
		15	99		
2	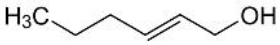 Trans-2-hexen-1-ol	15	33	100	142
		30	48		
		60	71		
		120	99		
3	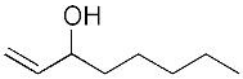 1-octene-3-ol	120	48	100	30
		240	76		
		480	83		
4	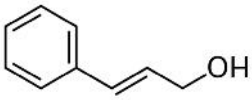 Cinnamyl alcohol	15	13	100	77
		60	69		
		120	78		
		180	81		

Reaction condition: 10 mmol substrate, 12 mmol TBHP, 5 mL chloroform, 0.1 g catalyst.
TOF is mmol of product/ mmol of vanadium in catalyst per hour.

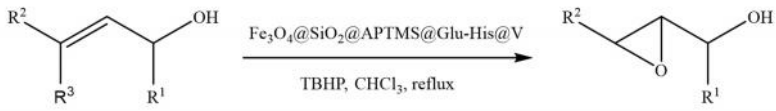

R^1: H, R^2: $CH_2CH_2CH_3$, R^3: H

R^1: H, R^2: Ph, R^3: H

R^1: $CH_2CH_2CH_2CH_2CH_3$, R^2: H, R^3: H

R^1: H, R^2: $CH_2CH_2CHC(CH_3)CH_3$, R^3: H

Scheme 3. Epoxidation reaction of the selected allyl alcohols.

The increasing reactivity trend of geraniol > *trans*-2-hexen-1-ol > 1-octene-3-ol > cinnamyl alcohol observed in the epoxidation reactions may be used as a criterion in gaining insight into the reaction mechanism. Since 99% of geraniol is converted to the corresponding epoxide in the presence of diphenylamine as a radical scavenger, it can be concluded that oxidation does not occur through a radical mechanism. More importantly,

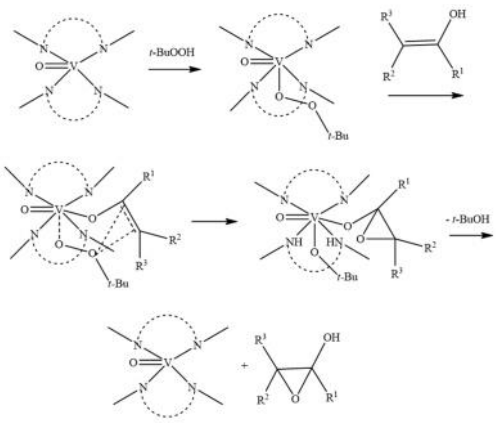

Scheme 4. Reaction mechanism for epoxidation of geraniol with catalyst.

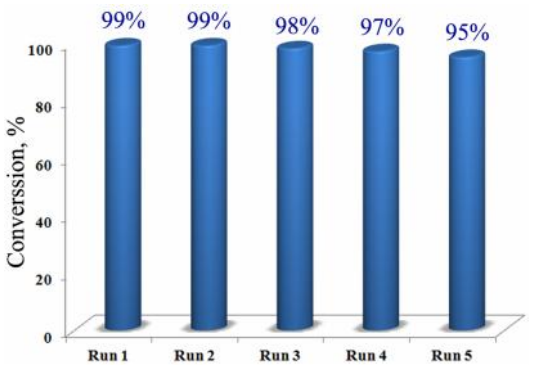

Figure 7. Reusability of catalyst. Reaction condition: 10 mmol substrate, 12 mmol TBHP, 5 mL chloroform, time 15 min and 0.1 g catalyst

since increasing the number of alkyl substituents of the double bond undergoing epoxidation from 1-octene-3-ol to geraniol (entry 3 to 1, Table 1) increases the reaction rate, it can be concluded that the insertion of the electrophilic oxygen into the double bond is concerted. As such, epoxidation reaction might have proceeded via the mechanism suggested by Conte [42] in which initial reaction of vanadium center with TBHP yields an alkylperoxovanadium complex (Scheme 4). Subsequently, reaction with allylic alcohol affords an alkoxo-alkylperoxovanadium complex. In the next step, an intramolecular oxygen transfer from O-O bond to double bond occurs, thus affording the corresponding coordinated epoxide. Finally, the catalyst is released with the formation of *t*-BuOH and epoxide product (Scheme 4). Based on the suggested mechanism, observation of the lowest rate for cinammyl alcohol containing a double bond conjugated to phenyl ring is expected (entry 4, Table 1).

Overall, high activity, selectivity, stability and reusability of the catalyst with no leaching during the reaction together with the easily magnetic recovery of the catalyst as well as fast reaction rates are some advantages of our catalysis system. Compared to the similar reported works on geraniol epoxidation in the presence of immobilized oxidovanadium(IV) acetylacetonate and $[VO(acac)_2]$APTES@K10 within 2 and 48 h, respectively [41-42], implementation of this reaction in catalyzed by Fe_3O_4@SiO_2@APTMS@Glu-His@V in lower reaction time seems promising.

Conclusion

Fe_3O_4@SiO_2@APTMS@Glu-His@V complex was prepared from modification of iron oxide nanomagnet particles followed by immobilization of glutaraldehyde-histidine Schiff base ligand and then complexation with $VOSO_4$. This compound was found to successfully catalyze the epoxidation of some allyl alcohols with TBHP in chloroform in moderate to high yields in short reaction times. It was also found that the catalyst can be reused four times without significant losing catalytic activity.

Acknowledgement

The financial support from Alzahra University is gratefully acknowledged.

References

1. Gupta K.C., Kumar Sutar A. Catalytic activities of Schiff base transition metal Complexes, *Coord. Chem. Rev.* **252:** 1420–1450 (2008).
2. Maurya M. R., Development of the coordination chemistry of vanadium through bis (acetylacetonato) oxovanadium(IV): synthesis, reactivity and structural aspects, *Coord. Chem. Rev.* **237:** 163-181(2003).
3. Licini G., Conteb V., Coletti A., Mbaa M., Zontaa C. Recent advances in vanadium catalyzed oxygen transfer reactions**,** *Coord. Chem. Rev.* **255:**2345– 2357 (2011).
4. Pillai S.- L., Subramanian S.-P., Kandaswamy M. A novel insulin mimetic vanadium flavonol complex: Synthesis, characterization and *in vivo* evaluation in STZ-induced rats, *Europ. J. Medicinal. Chem.* 63: **109-117**(2013).
5. Sanna D., Micera G., Garribba E. On the Transport of vanadium in blood serum, Inorg Chem, **52:** 11975−11985 (2013).
6. Rehder D. Biological and medicinal aspects of vanadium, *J. Inorg. Biochem.* **80:**81(2003).
7. Van de Velde F., Arends I. W.C.E., Sheldon R.A. Biocatalytic and biomimetic oxidations with Vanadium. Inorg Chem Commun **6**: 604–617(2000).
8. Maurya R.C., Rajput S. Oxovanadium(IV) complexes of bioinorganic and medicinal relevance: synthesis, characterization and 3D molecular modeling and analysis of some oxovanadium(IV) complexes involving the O, N-donor environment of pyrazolone-based sulfa drug Schiff bases. J Mol Struc**794:**24–34 (2006).
9. Pessoa J.C., Etcheverry S, Gambino D Vanadium compounds in medicine Coord. Chem. Rev. **301- 302**: 24-48 (2015).
10. Jia Y., Lu L., Zhu M., Yuan C., Xing S., Fu X.A. dioxidovanadium (V) complex of NNO-donor Schiff base as a selective inhibitor of protein tyrosine phosphatase 1B: synthesis, characterization, and biological activities Europ J Med Chem **128**: 287-292(2017).
11. Martins M.D.R.S., Atima M. F. Vanadium complexes: Recent progress in oxidation Catalysis, *Coord. Chem.* **301–302:**200–239 (2015).
12. Cornman C.R., Zovinka E.P., Meixner M.H. Vanadium (IV) complexes of an active site peptide of a protein tyrosine phosphatase, *Inorg. Chem.* **34**:5099-5100 (1995).
13. Chatt J., Dilworth J. R., Richards R. L. Recent Advances in the Chemistry of Nitrogen Fixation. *Chem. Rev.* **78:**589-625 (1978).
14. Crans D.C., Smee J.J., Gaidamauskas E., Yang L.Q. The

Chemistry and biochemistry of vanadium and the biological activities exerted by vanadium compounds. *Chem. Rev.* **104:** 849-902 (2004).

15. Thompson K.H., McNeill J.H., Orvig CVanadium Compounds as Insulin Mimics. *Chem. Rev.* **99:** 2561-2572 (1999).

16. Tasiopoulos A.J., Troganis A.N., Evangelou A., Raptopoulou C.P., Terzis A., Deligiannakis Y., Kabanos T.A. Synthetic analogues for oxovanadium(IV)–glutathione interaction: an EPR, synthetic and structure study of oxovanadium(IV) compounds with sulfhydryl containing pseudopeptides and dipeptides. *Chem. Eur. J.* **5:** 910-921(1999).

17. Schneider CJ, Penner-Hahn JE, Pecoraro VL. Elucidating the Protonation Site of Vanadium Peroxide Complexes and the Implications for Biomimetic Catalysis. J Am Chem Soc **130**: 2712-2713 (2008).

18. Ligtenbarg AGJ, Hage R, Feringa Ben L. Catalytic oxidations by vanadium Complexes, *Coord. Chem. Rev.* **237**: 89-101 (2003).

19. Gupta KC, Sutar AK, lin CP (2009) Polymer-supported Schiff base complexes in oxidation reactions. *Coord. Chem. Rev.* **253: 1926–1946.**

20. Yang Y, Zhang Y, Hao S, Guan J, Ding H, Shang F, Qiu P, Kan Q. Heterogenization of functionalized Cu(II) and VO(IV) Schiff base complexes by direct immobilization onto amino-modified SBA-15: Styrene oxidation catalysts with enhanced reactivity. Appl Catal A **381**: 274–281 (2010).

21. Maurya M R, Kumarb A, Costa Pessoab J. Vanadium complexes immobilized on solid supports and their use as catalysts for oxidation and functionalization of alkanes and alkenes, *Coord. Chem. Rev.* **255**: 2315– 2344 (2011).

22. Hu S., Liu D., Wang C., Chen Y., Guo., Borgna A., Yang Y. Liquid-phase epoxidation of *trans* stilbene and *cis*-cyclooctene over vanadium-exchanged faujasite zeolite catalyst Appl Catal A **386**: 74–82 (2010).

23. Maurya MR, Bisht M., Chaudhary N., Avecilla F., Kumar U., Hsu H.F. Synthesis, structural characterization, encapsulation in zeolite Y and catalytic activity of an oxidovanadium(V) complex with a tribasic pentadentate ligand. Polyhedron **54**:180–188 (2013).

24. Modi CK., Chudasama J.A., Nakum H.D., Parmar D.K., Patel A.L. Catalytic oxidation of limonene over zeolite-Y entrapped oxovanadium (IV) complexes as heterogeneous catalysts. J Mol Catal A Chem **395**: 151–161(2014).

25. Zamanifar E., Farzaneh F. Immobilized vanadium amino acid Schiff base complex on Al- MCM-41as catalyst for the epoxidation of allyl alcohols, *React Kinet, Mech Catal.* **104**:197– 209 (2011).

26. Yaul A.R., Pethe G.B., Aswar A.S. Russ J Coord Chem **36**: 254–258 (2010).

27. Sharpless KB, T.R. Verhoeven Metal-catalyzed, highly selective oxygenations of olefins and acetylenes with tert-butyl hydroperoxide. Practical considerations and mechanisms. Aldrichim. Acta **12:** 63–74(1979).

28. Masteri-Farahani M., Modarres M. Wells-Dawson heteropoly acid immobilized Inside the nanocages of SBA-16 with ship-in-a-bottle method: A new recoverable catalyst for the epoxidation of olefins, *J. Mol. Catal. A*: **417**:81-88 (2016).

29. Ooi Y.K., Yuliati L., Hartanto D., Nur H., Lee S.L. Mesostructured TUD-C supported molybdena doped titania as high selective oxidative catalyst for olefins epoxidation at ambient condition, *Micropor Mesopor Mater* **225**: 411–420 (2016).

30. M. Lin, C. Xia, B. Zhu, H. Li, X. Shu, Green and efficient epoxidation of propylene with hydroge peroxide (HPPO process) catalyzed by hollow TS-1 zeolite: A 1.0 kt/a pilot-scale study, *Chem Engin J* **295**: 370–375 (2016).

31. Masteri-Farahani M., Niakan M. Heterogenization of peracids onto the MCM-41 and SBA-16 mesoporous materials for the epoxidation of cyclooctene. *Mater Chem Phys* **195**: 74-81(2017).

32. Mavrogiorgou A., Baikousi M., Costas V., Mouzourakis E., Deligiannakis Y., Karakassides M.A., Louloudi M. Mn-Schiff base modified MCM-41, SBA-15 and CMK-3 NMs as single-site heterogeneous catalysts: Alkene epoxidation with H2O2 incorporation, *J. Mol. Catal. A:* **413**: 40–55(2016).

33**.** Andrade A.L., Souza D.M., Pereira M. C., Fabris J. D. Domingues R. Z. Synthesis and characterization of magnetic nanoparticles coated with silica through a sol-gel approach. Cerâmica **55**: 420-424 (2009).

34. Liu X., Ma Z., Xing J., Liu H. Preparation and characterization of amino–silane modified superparamagnetic silica nanospheres. J Magn Magn. Mater **270**: 1–6 (2004).

35. Sahooa P.C., Janga Y.N., Leea S. W., Immobilization of carbonic anhydrase and an artificial Zn(II) complex on a magnetic support for biomimetic carbon dioxide sequestration. *J. Mol. Catal.* B **82**:37– 45(2012).

36. Farzaneh F., Rashtizadeh E., A new Cu Schiff base complex with histidine and glutaraldehyde immobilized on modified iron oxide nanoparticles as a recyclable catalyst for the oxidative homocoupling of terminal alkynes, J Iran Chem Soc 13:1145–1154(2016).

37. Farzaneh F., Sadeghi Y. Immobilized V-MIL-101 on modified Fe_3O_4 nanoparticles as heterogeneous catalyst for epoxidation of allyl alcohols and alkenes. *J. Mol. Catal. A* **398**: 275–281 (2015).

38. Hamidipour L, Farzaneh F. Immobilized VOsalpr on modified Fe3O4nanoparticles as a magnetically separable epoxidation catalyst. CR Chimie,**17**: 927-933(2014).

39. Hamidipour L, Farzaneh F, Ghandi M. Immobilized $Co(acac)_2$ on modified Fe3O4 nanoparticles as a magnetically separable epoxidation catalyst. Reac Kinet Mech Catal **107**:421- 433(2014).

40. Asgharpour Z., Farzaneh F., Abbasi A. Synthesis, characterization and immobilization of a new cobalt (II) complex on modified magnetic nanoparticles as catalyst for epoxidation of alkenes and oxidation of activated alkanes. *RSC Adv* **6**: 95729- 95739(2016).

41. Dorbes S, Pereira C, Andrade M, Barros D, Pereira AM, Rebelo SLH, Araújo JP, Pires J, Carvalho AP,Freire COxidovanadium(IV) acetylacetonate immobilized onto CMK-3 for heterogeneousepoxidation of geraniol, *Micropor. Mesopor. Mater.* **160**: 67-74 (2012).

42. Conte V., Di Furia F., Licini G., Liquid phase oxidation reactions by peroxides in th presence of vanadium complexes. Appl Catal A **157**:335–361(1997).